Efficient Ligation of the *Schistosoma* Hammerhead Ribozyme†

Marella D. Canny, Fiona M. Jucker, and Arthur Pardi*

Department of Chemistry and Biochemistry, University of Colorado at Boulder, Boulder, Colorado 80309-0215

Received October 5, 2006; Revised Manuscript Received January 11, 2007

ABSTRACT: The hammerhead ribozyme from *Schistosoma mansoni* is the best characterized of the natural hammerhead ribozymes. Biophysical, biochemical, and structural studies have shown that the formation of the loop−loop tertiary interaction between stems I and II alters the global folding, cleavage kinetics, and conformation of the catalytic core of this hammerhead, leading to a ribozyme that is readily cleaved under physiological conditions. This study investigates the ligation kinetics and the internal equilibrium between cleavage and ligation for the *Schistosoma* hammerhead. Single turnover kinetic studies on a construct where the ribozyme cleaves and ligates substrate(s) in *trans* showed up to 23% ligation when starting from fully cleaved products. This was achieved by an ∼2000-fold increase in the rate of ligation compared to a minimal hammerhead without the loop−loop tertiary interaction, yielding an internal equilibrium that ranges from 2 to 3 at physiological Mg^{2+} ion concentrations (0.1−1 mM). Thus, the natural *Schistosoma* hammerhead ribozyme is almost as efficient at ligation as it is at cleavage. The results here are consistent with a model where formation of the loop−loop tertiary interaction leads to a higher population of catalytically active molecules and where formation of this tertiary interaction has a much larger effect on the ligation than the cleavage activity of the *Schistosoma* hammerhead ribozyme.

Ribozymes are the catalytic molecules that take part in a variety of biochemical reactions including peptidyl transfer (*1*, *2*), self-splicing (*3*−*5*), tRNA maturation (*6*, *7*), regulation of translation in Gram-positive bacteria (*8*), and processing of replication intermediates in plant pathogenic RNAs such as viroids and satellite RNAs of viruses (*9*−*11*). These plant pathogenic RNAs replicate via a rolling circle mechanism where hammerhead and hairpin ribozymes self-cleave the long multigenomic RNA strand into single genomes (*11*−*15*). These linear single genomes must be subsequently recircularized to continue the replication cycle. The hammerhead ribozyme has been proposed to also function as the RNA ligase where it reacts in *cis* on a linear RNA to give the circular genome (*11*, *16*−*18*). Other possibilities for the in vivo ligation reaction are that the ribozyme requires the assistance of a host protein (*19*) or that a host protein performs the ligation reaction (*20*−*22*).

The hammerhead ribozyme belongs to the group of small catalytic RNAs that includes the hairpin, VS,[1] and HDV ribozymes (*23*). These ribozymes catalyze the same cleavage reaction where nucleophilic attack of the 2′-OH at the cleavage site phosphate leads to products containing a 2′,3′-cyclic phosphate and a 5′-OH (*11*, *24*). The minimal hammerhead ribozyme consists of a three-helix junction that folds into a Y-shaped structure surrounding a 15-nucleotide catalytic core where 11 of these nucleotides are conserved in all hammerhead sequences (*15*, *24*, *25*). This minimal hammerhead has been extensively studied by biochemical, biophysical, and structural techniques (*26*), and efficient cleavage activity in vitro is achieved only at relatively high levels of Mg^{2+} ions (cleavage rate constants of ∼1.0 min^{-1} at 10 mM Mg^{2+}) (*27*). Although this minimal hammerhead exhibits ligation activity in vitro, cleavage is highly preferred, with the ratio of fraction cleaved to uncleaved of ∼130 (*27*). More recent studies have shown that when the minimal sequence of the hammerhead ribozyme is extended to include naturally occurring loop−loop tertiary interactions between stems I and II (Figure 1), catalysis takes place under physiological conditions both in vivo and in vitro (*28*, *29*). This loop−loop tertiary interaction stabilizes the catalytically active conformation (*30*), which increases observed cleavage rate constants by up to 50-fold, allowing efficient cleavage even at low concentrations of metal ions [cleavage rate constants of ∼0.2−1.4 min^{-1} in 100 μM Mg^{2+} (*28*, *31*, *32*)].

The hammerhead ribozyme from the *Schistosoma mansoni* satellite DNA (*33*, *34*) is the best characterized of the natural hammerhead systems with data on the cleavage kinetics, global folding by FRET, local and global dynamics by EPR, and cross-linking studies (*31*, *35*−*39*). These studies have shown that the formation of the loop−loop tertiary interaction alters the structure, populations of active conformations, global folding, and cleavage kinetics of the natural hammerhead, leading to a ribozyme that is readily cleaved under physiological conditions. In addition, Scott and co-workers have solved the X-ray structure of a construct of the *S.*

† This work was supported in part by grants from the NIH (AI 30726) and the W. M. Keck Foundation initiative in RNA science at the University of Colorado, Boulder.

* To whom correspondence should be addressed. E-mail: arthur.pardi@colorado.edu. Phone: (303) 492-6263. Fax: (303) 492-2439.

[1] Abbreviations: VS, *Neurospora* varkud satellite RNA; HDV, hepatitis delta virus; FRET, fluorescence resonance energy transfer; EPR, electron paramagnetic resonance; (−)sTRSV, negative strand of the satellite RNA of tobacco ringspot virus; PAGE, polyacrylamide gel electrophoresis; EDTA, ethylenediaminetetraacetic acid; Tris-HCl, tris(hydroxymethyl)aminomethane hydrochloride; ASBVd(+), positive strand of avocado sunblotch viroid; ASBVd(−), negative strand of avocado sunblotch viroid.

10.1021/bi062077r CCC: $37.00
Published on Web 02/24/2007

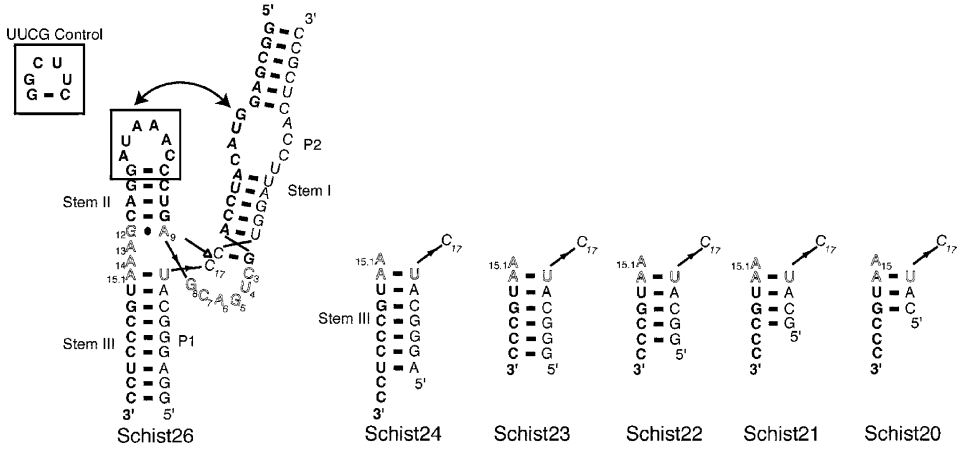

FIGURE 1: Sequence and secondary structure of the *trans Schistosoma* hammerhead ribozyme constructs. The full construct is shown for Schist26, whereas only stem III and the corresponding P1 are shown for Schist24 through Schist20 since the rest of the construct is identical to Schist26. Construct names correspond to the number of bases in the substrate strand. The double-headed arrow indicates the tertiary loop−loop interaction between stems I and II. Canonical base pairs are shown as solid lines, and the Hoogsteen base pair is shown with a "•". The conserved nucleotides that make up the catalytic core are shown in outline and numbered according to standard convention. Bold nucleotides indicate the ribozyme strand, and the single-headed arrow points to the scissile bond. The cleavage experiments employ a two-stranded construct consisting of the ribozyme and the full-length substrate. The ligation experiments employ a three-stranded construct consisting of the ribozyme, the 5′-cleavage product, P1, which has a 2′,3-cyclic phosphate at C_{17}, and the 3′-cleavage product, P2, which has a 5′-OH on C_{18}. For the UUCG control, the sequence in the stem II loop is replaced with a UUCG sequence (boxed).

mansoni hammerhead ribozyme, which contains the natural loop−loop tertiary interaction (*40*). This structure shows large conformational changes in the catalytic core compared to the structure of the minimal hammerhead ribozyme and represents an improved model for understanding the catalytic mechanism of the hammerhead ribozyme (*30*, *40*).

The cleavage reaction for several natural hammerhead ribozymes has been studied (*28*, *29*, *32*), but the ligation kinetics have only been characterized for the sTRSV hammerhead (*32*). Here we report on the ligation kinetics and internal equilibrium of the best characterized hammerhead, the *Schistosoma* ribozyme. This *Schistosoma* construct is an efficient ligase and yields up to 23% ligated product starting from the fully cleaved substrate, which is the highest level of ligation reported for any unmodified hammerhead. This *Schistosoma* ribozyme shows an ~2000-fold increase in the rate of ligation compared to the minimal hammerhead and has a K_{eq}^{int} between 2 and 3 at physiological Mg^{2+} concentrations. Thus the loop−loop tertiary interaction leads to a ribozyme that is both an efficient nuclease and ligase in vitro.

MATERIALS AND METHODS

RNA Synthesis and Sample Preparation. A set of *S. mansoni* hammerhead (*33*, *34*) ribozyme constructs were employed that differ primarily in the length of stem III (Figure 1). The cleavage constructs consist of two RNA strands, a ribozyme strand and a substrate strand, whereas the ligation construct consists of the ribozyme strand and the two cleavage products, P1 and P2. RNAs were either chemically synthesized (W. M. Keck Facility, Yale University, and Dharmacon Inc.) or generated by in vitro transcription using T7 RNA polymerase (*41*). Synthetic DNA templates for in vitro transcription were purchased from Integrated DNA Technologies. Transcription products were purified by 20% (w/v) denaturing PAGE, and full-length RNAs were excised from the gel, eluted, and ethanol precipitated. The RNAs were dissolved in excess EDTA (10 mM), heated to 65 °C for 5 min to remove any Mg^{2+} ions, and cooled at room temperature for 10 min. All RNAs were exchanged into reaction buffer containing 50 mM Tris-HCl, pH 7.0, 100 mM NaCl, and 0.1 mM EDTA by repeated dilution/concentration in Microcon YM-3 centrifugal filter devices (Millipore) to remove the excess EDTA.

The substrate strands were 5′-^{32}P end-labeled using T4 polynucleotide kinase and purified by 20% (w/v) denaturing PAGE. To obtain ^{32}P-labeled P1, which has the 2′,3′-cyclic phosphate required for the ligation reaction, full-length ^{32}P-labeled substrate was annealed to a 10-fold excess of ribozyme by heating to 70 °C and then cooling to 25 °C over 10 min. Cleavage of the substrate strand was initiated by addition of $MgCl_2$ to a final concentration of 20 mM Mg^{2+}, and the reaction was allowed to cleave at 25 °C for 20 min. The reaction was then heated to 70 °C, slowly cooled, and allowed to cleave at 25 °C for 20 min. This cycle was repeated two more times to achieve nearly 100% cleavage, and then ^{32}P-P1 was gel purified, as described above. The unlabeled P1 that was employed as the chase in dissociation reactions and P2 were chemically synthesized, and both RNAs have a terminal OH at their 3′ and 5′ ends.

The buffers were purified over chelating resin (iminodiacetic acid; Sigma) to remove any trace of Mg^{2+} or other divalent metal ions. The stock solutions of buffer, $MgCl_2$, and NaCl were analyzed for contaminating metals by inductively coupled plasma optical emission spectroscopy.

Ligation and Cleavage Experiments. Single turnover ligation experiments were performed by first combining 0.5 μM ribozyme strand, 1 μM P2, and trace ^{32}P-P1 in 110 μL of reaction buffer, heating to 70 °C for 2 min, and cooling to 25 °C over 10 min. The ligation reactions were then initiated by the addition of $MgCl_2$ to the indicated final concentrations. At times ranging from 8 s to 20 min, samples were removed and quenched in 80% formamide, 0.02% bromophenol blue, and excess EDTA and immediately frozen on dry ice. The reaction products were separated by 20% (w/v) denaturing PAGE. ^{32}P radioactivity of both ligated and unligated bands was quantified by phosphorimager analysis

using a Typhoon 9400 variable mode imager and ImageQuant 5.2 software (Amersham Biosciences). The observed ligation rate constants were determined with KaleidaGraph 3.5 (Synergy Software), where the fraction of ^{32}P-labeled ligated full-length substrate versus time was fit to the equation $F_t = F_0 + F_\infty(1 - e^{-kt})$, where F_t is the fraction of the full-length substrate at time t, F_0 is the initial fraction of full-length substrate, F_∞ is the maximum fraction of full-length substrate, and k is the observed rate constant.

For experiments where the observed rates were too fast to measure manually, a KinTek chemical quench-flow model RQF-3 instrument was used. These experiments were performed at room temperature by first annealing the ribozyme strand, a 2-fold excess of P2, and trace ^{32}P-P1 as described above. Ligation was initiated by rapidly mixing (2 ms dead time) ~15 μL of annealed hammerhead with ~15 μL of 2× Mg^{2+} in reaction buffer, followed by a rapid quench with 90 μL of gel loading buffer (80% formamide, excess EDTA, and 0.02% bromophenol blue). The radioactively labeled reaction products were resolved by 20% denaturing PAGE and quantified by phosphorimager analysis as above.

Single turnover cleavage experiments were performed under the same conditions and analyzed by the same procedure as the ligation experiments except that trace full-length ^{32}P-labeled substrate was annealed to the 0.5 μM ribozyme strand.

Measurement of P1 Dissociation Rate Constants. Pulse−chase experiments were used to measure P1 dissociation rate constants (*27*) where 1 μM ribozyme strand, 2 μM P2, and trace ^{32}P-P1 were annealed as described above. Schist21 and Schist 23 P1s were annealed to the Schist23 ribozyme strand whereas Schist24 and Schist26 P1s were annealed to the Schist26 ribozyme strand. P2 was identical for all experiments. The annealed hammerheads were incubated in reaction buffer containing 1 mM Mg^{2+} for 30 min at room temperature. Unlabeled P1 (50 μM) was then added to initiate the chase reaction. Aliquots were removed at various times, added to 2 μL of native gel loading buffer (50% sucrose, 0.02% each bromophenol blue and xylene cyanol), and then immediately loaded on a running 12% native polyacrylamide gel containing 1 mM Mg^{2+}. The fraction of ^{32}P-P1 complexed to the ribozyme was quantified by phosphorimager analysis, and the P1 dissociation rate constant was determined by fitting the fraction of complexed ^{32}P-P1 versus time as described above.

RESULTS AND DISCUSSION

Ligation and Internal Equilibrium in the Schistosoma Hammerhead Ribozyme. The hammerhead ribozyme is involved in rolling circle replication of circular RNA genomes, where it cleaves replicated mulitmeric genomes into monomeric genomes (*9*, *11*, *13*−*15*). The hammerhead is also thought to recircularize these RNAs through the reverse ligation reaction (*11*, *16*−*18*) (Figure 2). We previously reported the observed cleavage rate constant ($k_{obs,cleave}$) for a *trans* construct of the *Schistosoma* hammerhead ribozyme as a function of Mg^{2+} concentration and pH (*31*). The ligation activity and the internal equilibrium of this hammerhead are studied here. For these studies the previously characterized *trans Schistosoma* construct (Schist23, Figure 1) was extended by three base pairs in stem III (Schist26, Figure 1) to reduce dissociation of P1 from the ribozyme strand during the lifetime of the experiment (see below). Figure 3 shows a ligation experiment on Schist26 in 10 mM Mg^{2+} at 25 °C under single turnover conditions. This ligation reaction plateaus at ~23% ligated substrate, which is a higher level of ligation than previously reported for other hammerhead constructs (*27*, *32*, *39*). This indicates that the ligation reaction of the *Schistosoma* hammerhead is quite efficient in vitro, where a significant percentage of a cleaved substrate can religate. The kinetic data in Figure 3B are fit well by a single exponential, yielding an observed rate constant for ligation, $k_{obs,ligate}$, of ~26 min^{-1}. Ligation experiments were performed on Schist26 at various Mg^{2+} concentrations, yielding $k_{obs,ligate}$ ranging from 1.5 to 74 min^{-1} in 0.5−50 mM Mg^{2+} (Table 1). Cleavage experiments were also performed on Schist26 starting from the full-length substrate. In the Schist26 construct, k_{obs} represents the approach to equilibrium and thus the sum of k_{cleave} and k_{ligate}. Therefore, $k_{obs,cleave}$ should equal $k_{obs,ligate}$ for the same reaction conditions, and as seen in Table 1, within error these

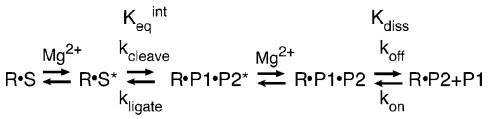

FIGURE 2: Reaction scheme of the *trans* hammerhead ribozyme cleavage and ligation reaction. R is the ribozyme strand, S is the substrate strand, and P1 and P2 are the 5′- and 3′-cleavage products, respectively. k_{cleave} is the cleavage rate constant, k_{ligate} is the ligation rate constant, k_{off} is the P1 dissociation rate constant, k_{on} is the P1 association rate constant, K_{eq}^{int} is the equilibrium constant for the cleavage−ligation step of the reaction, and K_{diss} is the equilibrium constant for dissociation of P1. The asterisks indicate the catalytically active forms of the cleaved and ligated complexes.

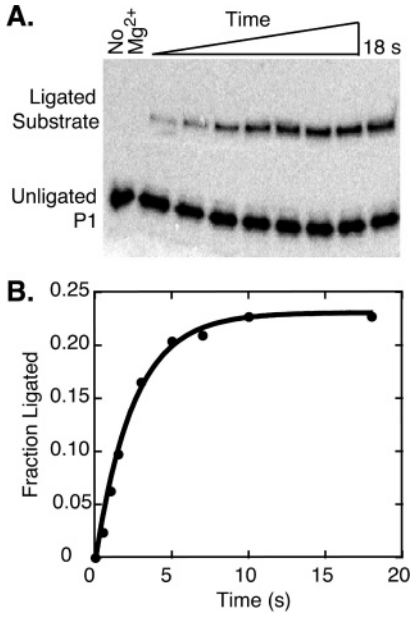

FIGURE 3: Single turnover ligation kinetics of the Schist26 hammerhead ribozyme. (A) A 20% denaturing polyacrylamide gel used to separate ^{32}P-labeled ligated full-length substrate from ^{32}P-P1 in the ligation experiment for Schist26 in 10 mM Mg^{2+}. The different lanes correspond to samples removed from the ligation reaction at various times after addition of Mg^{2+}. (B) Plot of the fraction of ligated substrate vs time where the solid line shows the fit to a single exponential with a $k_{obs,ligate}$ of ~26 min^{-1}.

Table 1: Mg^{2+} Dependence of the Rate Constants and Internal Equilibrium Constants for the Internal Equilibrium of the *Schistosoma* Hammerhead Ribozyme[a]

Mg^{2+} (mM)	Schist26 $k_{obs,cleave}$ (min^{-1})	Schist26 $k_{obs,ligate}$ (min^{-1})	Schist21 k_{cleave} (min^{-1})	k_{ligate} (min^{-1})[b]	K_{eq}^{int} [c]	K_{eq}^{int} [d]
0.1	0.2	nd	0.13	0.07 ± 0.05	1.9 ± 0.7	≥ 1.3
0.5	3	1.5	2.1	0.9 ± 0.7	2.3 ± 0.8	1.3−47
1	5.9	2.7	4.4	1.5 ± 1.5	2.9 ± 1.0	1.3−16
5	30	16	9.4	20 ± 6	0.5 ± 0.4	0.5−3.3
10	40	26	23	17 ± 9	1.4 ± 0.6	0.5−3.2
15	46	45	27	19 ± 11	1.4 ± 0.6	0.5−3.0
25	74	60	33	41 ± 16	0.8 ± 0.4	0.5−3.0
50	120	74	42	78 ± 25	0.5 ± 0.4	0.5−3.4

[a] $k_{obs,cleave}$, $k_{obs,ligate}$, and k_{cleave} all have errors of less than ±20% based on replicate experiments. The errors for k_{ligate} and K_{eq}^{int} (calculated from k_{cleave}/k_{ligate}) were determined from standard error propagation assuming 20% errors for $k_{obs,cleave}$ and k_{cleave}. [b] k_{ligate} was calculated by subtracting k_{cleave} of Schist 21 from $k_{obs,cleave}$ of Schist26. $k_{obs,cleave}$ was used for this calculation instead of $k_{obs,ligate}$ to eliminate the additional complication that ligation experiments start with three strands instead of two strands. [c] Calculated from k_{cleave}/k_{ligate}. [d] Range of values calculated from the fraction of cleaved substrate in the cleavage and ligation experiments of Schist26, assuming 100% active RNA (see text).

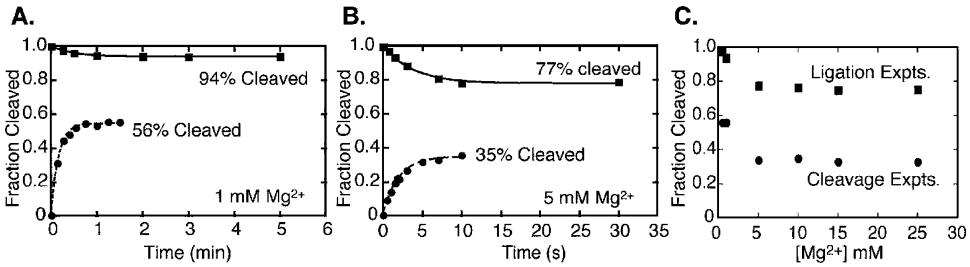

FIGURE 4: Fraction of cleaved substrate in cleavage and ligation experiments. Plots of the fraction of cleaved substrate vs time from the cleavage (circles) and ligation (squares) experiments in (A) 1 mM Mg^{2+} and (B) 5 mM Mg^{2+}. (C) Maximum fraction of cleaved substrate observed in the cleavage experiments used to determine $k_{obs,cleave}$ (circles) and in the ligation experiments used to determine $k_{obs,ligate}$ (squares) at varying Mg^{2+} concentrations.

observed rate constants are within a factor of 2 for all Mg^{2+} concentrations.

Several methods were next used to estimate the internal equilibrium (K_{eq}^{int}) between cleavage and ligation in vitro for the *Schistosoma* hammerhead construct. In one approach, limits on K_{eq}^{int} were calculated from the final fraction of cleaved substrate in the ligation or cleavage experiments. Panels A and B of Figure 4 show the fraction of cleaved substrate versus time starting from the fully cleaved and fully ligated substrates in 1 and 5 mM Mg^{2+}, respectively. If all of the substrates and ribozymes are fully active, then at equilibrium (i.e., when fraction cleaved plateaus) the fraction of cleaved substrate should be identical when initiated from either side of the reaction. This is not the case for Schist26, where the fractions of cleaved substrate at the plateaus differ by ~40% between the cleavage and ligation experiments at every Mg^{2+} concentration (Figure 4C). These data indicate that, as is the case with many RNAs (*42*−*45*), Schist26 has a significant, long-lived inactive population, and the conversion between these inactive and active species is slow compared to the cleavage and ligation rates (see below).

Despite the complications of an inactive population, the plateaus of the kinetic experiments provide upper and lower limits for K_{eq}^{int} (=fraction cleaved/fraction ligated). For example, at 1 mM Mg^{2+} (Figure 4A), 56% of the substrates were cleaved which means that at least 56% of the species are active and cleavable, and these data yield a lower limit on K_{eq}^{int} of 1.3. Similarly, the plateau for the ligation reaction was 94% cleaved substrate, which leads to an upper limit on K_{eq}^{int} of 16. Using the same rationale for the data at 5 mM Mg^{2+} (Figure 4B) gives a range of $0.5 \leq K_{eq}^{int} \leq 3.3$. The ranges for K_{eq}^{int} determined by this method at the various Mg^{2+} concentrations are given in Table 1. There are larger ranges for K_{eq}^{int} at the lower Mg^{2+} concentrations, which arise from the low level of ligated product in the ligation experiments under these conditions (Figure 4C).

A second approach was employed that calculates K_{eq}^{int} from the ratio of the cleavage and ligation rate constants, k_{cleave}/k_{ligate}. If the rate constant for conversion of inactive to active molecules is much slower than k_{cleave} or k_{ligate}, then the measured rates are not affected by the presence of such long-lived, inactive populations. A cleavage-only construct, Schist21 (Figure 1), was designed with a shorter P1 so that the rate of dissociation of P1 is much faster than the ligation rate (see below). Thus k_{obs} is assumed to be equal to k_{cleave} for this construct and was measured as a function of Mg^{2+} concentration. The measured k_{cleave} is then subtracted from $k_{obs,cleave}$ for Schist26, giving k_{ligate}, which is then used to calculate K_{eq}^{int} ($=k_{cleave}/k_{ligate}$) (Table 1). This method yields K_{eq}^{int} values between 0.5 and 3 over the entire range of Mg^{2+} concentrations, which fall within the limits determined from the cleavage plateaus. Table 1 shows that although there are very large changes in the cleavage and ligation rates as a function of Mg^{2+}, there are relatively small changes in K_{eq}^{int}. For these data the ratio of the rate constants is a better method for estimating K_{eq}^{int} than using the plateaus of the cleavage and ligation reactions. This is because the calculation of the fraction of cleaved or ligated substrate at the plateaus is directly affected by the long-lived, inactive population, whereas k_{cleave} or k_{ligate} is not since, as shown below, the conversion from inactive to active species is much slower than the rates of cleavage or ligation.

Analysis of the Mg^{2+} dependence of $k_{obs,cleave}$ for Schist26 and k_{cleave} for Schist21 yields fits for $[Mg^{2+}]_{1/2}$ of ~55 and

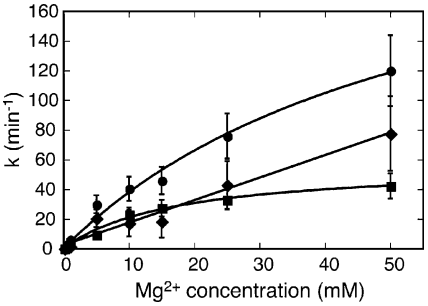

FIGURE 5: Mg^{2+} dependence of the kinetics for the Schist26 and Schist21 constructs. A plot of $k_{obs,cleave}$ for Schist26 (circles), k_{cleave} for Schist21 (squares), and calculated k_{ligate} (diamonds) vs Mg^{2+} concentration. For $k_{obs,cleave}$ and k_{cleave} the lines are fits of the Mg^{2+} dependence of the rate constant, k, to a two-state model for Mg^{2+} binding using the equation $k = k_{max}[Mg^{2+}]/([Mg^{2+}] + [Mg^{2+}]_{1/2})$, where k_{max} is the rate constant at saturating Mg^{2+} and $[Mg^{2+}]_{1/2}$ is the Mg^{2+} concentration required to achieve half of the maximal cleavage rate constant. This analysis assumes a Hill coefficient of 1 since there was no evidence for cooperative binding of Mg^{2+} for any of the kinetic data. These fits yield $[Mg^{2+}]_{1/2}$ of 55 ± 10 mM for $k_{obs,\ cleave}$ for Schist26 and 17 ± 3 mM for k_{cleave} for Schist21. The k_{ligate} does not saturate at the Mg^{2+} concentrations employed here, making it impossible to determine a $[Mg^{2+}]_{1/2}$. Thus for k_{ligate} the solid line is a simple linear fit of k_{ligate} with $[Mg^{2+}]$. The error bars are based on a 20% error between replicate experiments for the measured rate constants (see Table 1).

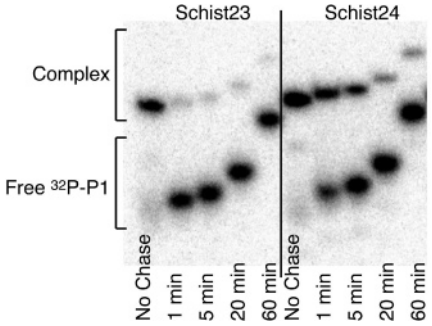

FIGURE 6: Native polyacrylamide gels of ^{32}P-labeled P1 for pulse−chase experiments used to measure rate constants for P1 dissociation from the ribozyme complex in 1 mM Mg^{2+}. The times indicate when the sample was loaded on the gel after the unlabeled chase was added to the reaction. The samples were loaded on a running gel, so the bands are shifted up in the gel for the longer time points. The left half of the gel is data for the P1 of Schist23 dissociating from the Schist23 ribozyme, and the right half of the gel is for the P1 of Schist24 dissociating from the Schist26 ribozyme (see Materials and Methods).

~17 mM, respectively, where $[Mg^{2+}]_{1/2}$ is the concentration of Mg^{2+} required to reach half of the maximum observed cleavage rate (Figure 5). k_{ligate} does not saturate at the concentrations of Mg^{2+} tested here, indicating a higher value of $[Mg^{2+}]_{1/2}$ for the ligation than the cleavage reaction. There was no evidence for cooperative binding of Mg^{2+} in either reaction. These results indicate that at concentrations of Mg^{2+} >30 mM the rate-limiting step in the cleavage reaction is independent of Mg^{2+}. However, the rate-limiting step in the ligation reaction shows a Mg^{2+} dependence even for the highest Mg^{2+} concentrations used here.

One potential problem in employing the cleavage-only (Schist21) construct is that the measured cleavage rates could be affected by having only four base pairs in stem III, so that this helix may not be stably formed. To address this, the cleavage rates were also measured for the Schist20 and Schist22 substrates in 0.1, 0.5, and 1.0 mM Mg^{2+}. The k_{obs} for cleavage of Schist 21 and Schist22 is the same within error at each Mg^{2+} concentration (data not shown). These results demonstrate that only four base pairs in stem III are needed for full cleavage activity of the *Schistosoma* hammerhead ribozyme. This agrees with previous studies by Hertel et al. on the minimal hammerhead HH16 where four base pairs in stem III were also required for full cleavage activity (*46*). In contrast, Schist20 (which only forms three base pairs in stem III) had k_{obs} values that were ~20-fold smaller than those of Schist21 and Schist22. Combined with the studies of the dissociation kinetics of P1 in the various constructs (see below), these results provide strong evidence that $k_{obs} = k_{cleave}$ for the Schist21 construct.

Dissociation Kinetics of P1 from the Ribozyme Complex. The Schist21 and Schist26 constructs were designed so that the dissociation of P1 was either much faster or much slower than k_{obs}, respectively. To test this assumption, pulse−chase experiments (*27*) were performed with a variety of substrates that contain between four (Schist21) and nine (Schist26) base pairs in stem III (see Figure 1). Schist26 has the longest P1 and is expected to have the smallest dissociation rate constant, $k_{off,P1}$. The pulse−chase experiment on Schist26 showed that P1 dissociates very slowly, with less than 10% dissociated after 24 h, which corresponds to $k_{off,P1} < 7 \times 10^{-5}$ min^{-1} (data not shown). This $k_{off,P1}$ is over 1000 times smaller than the smallest $k_{obs,\ cleave}$ measured for this construct (0.2 min^{-1} in 0.1 mM Mg^{2+}), meaning that the cleavage/ligation reaction is much faster than P1 dissociation. Estimates for k_{off} can also be obtained from the K_{diss} for RNA duplex formation [which is calculated using nearest neighbor rules (*47*)] and the association rate constant, k_{on}, because $k_{off} = K_{diss}k_{on}$. The k_{on} has been shown to be relatively independent of the length and the sequence of the RNA for short duplexes (*48*), and a k_{on} of 1.3×10^8 M^{-1} min^{-1} was used here (*27*). The nearest neighbor calculations for the nine base pair stem III of Schist26 gives a K_{diss} of 4×10^{-14} M, which then yields a $k_{off,P1}$ of 5.2×10^{-6} min^{-1}. Thus, the measured and predicted rate constants for the P1 of Schist26 clearly demonstrate that product dissociation of P1 will not affect the measured cleavage/ligation data for this construct.

Pulse−chase experiments were also performed on Schist24 and Schist23 (Figure 6) and yielded $k_{off,P1}$ values of 0.5 and >2 min^{-1}, respectively. These are similar to the values predicted using nearest neighbor calculations, which give $k_{off,P1}$ values of 0.1 min^{-1} for Schist24 and 3.5 min^{-1} for Schist23 and demonstrate the validity of this method for predicting the dissociation rates for P1. The good agreement between the measured and the predicted values for $k_{off,P1}$ for the Schist23 and Schist24 constructs means that this natural hammerhead ribozyme does not hold on to the 5′ product (P1) with higher affinity than expected from simple duplex formation in stem III. This is in contrast to the four-way junction hairpin ribozyme that binds its 3′-cleavage product with ~50-fold higher affinity relative to the minimal hairpin (*49*). The P1 of Schist21 is predicted to dissociate very rapidly with $k_{off,P1}$ of 4.5×10^4 min^{-1}, which is 1000 times faster than the fastest k_{obs} measured for this construct (42 min^{-1} in 50 mM Mg^{2+}). This is consistent with ligation experiments that showed no measurable ligation for Schist21 (data not shown). These results show that the P1 for Schist21 dissociates before the ligation reaction can occur, confirming

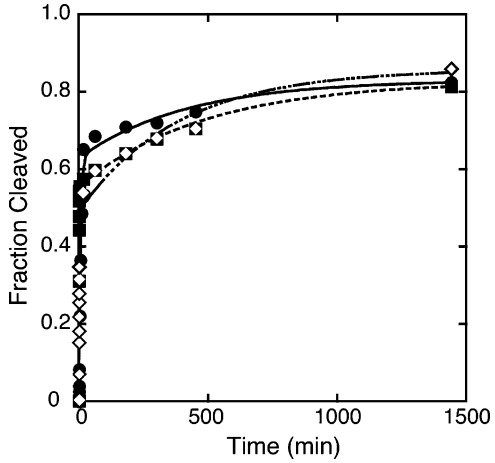

FIGURE 7: Single turnover cleavage kinetics followed for 24 h to monitor conversion of inactive to active species for Schist26. A plot of the fraction of cleaved substrate vs time is shown for cleavage experiments in 0.1 mM (circles), 1 mM (squares), and 10 mM (open diamonds) Mg^{2+}. The plots are a combination of the cleavage data from the 24 h experiments and from the manual and quench flow experiments. The data are fit to a double exponential, where one exponential corresponds to the cleavage/ligation kinetics and the second exponential corresponds to kinetics for the conversion of inactive to active ribozymes. The fit to the second exponential yields $k_{\text{inactive}\rightarrow\text{active}}$ of $\sim$0.006 min^{-1}.

that the k_{obs} for Schist21 is only measuring the cleavage and not the ligation kinetics.

Inactive Populations. RNAs are well-known to form alternate/multiple conformations, and this property can complicate the interpretation of kinetic or biochemical experiments (*42*, *45*). In the case of this *Schistosoma* hammerhead, starting from either the fully cleaved or fully ligated substrates does not lead to the same populations of cleaved product (Figure 4), indicating a significant population of inactive species. Furthermore, it cannot be assumed that the inactive population is the same coming from either direction especially since the ligation reaction starts with three RNA strands and the cleavage reaction with only two strands. To test whether the inactive species in the cleavage construct could convert over time to active species, cleavage experiments were followed for 24 h on Schist26 in 0.1, 1, and 10 mM Mg^{2+}. Figure 7 shows the cleavage data from the 24 h experiments combined with data from the manual and quench flow experiments under the same conditions. After 24 h $\sim$80% of the substrate is cleaved at all three Mg^{2+} concentrations. The pulse−chase experiments on the Schist26 ribozyme showed that a small fraction (<10%) of this 80% is potentially due to P1 dissociation. Thus using 70% cleaved gives a K_{eq}^{int} of $\sim$2.3, which is similar to the K_{eq}^{int} calculated from the kinetic data.

The kinetic data from the 24 h experiments (Figure 7) can be used to determine an apparent rate constant for the conversion of inactive to active ribozyme and yields a $k_{\text{inactive}\rightarrow\text{active}}$ of 0.006 ± 0.003 min^{-1}. Such a slow conversion to active ribozymes indicates that the inactive, long-lived population does not affect the observed rate constants for the cleavage/ligation experiments discussed above.

The k_{obs} for the cleavage and ligation experiments represents the approach to equilibrium and thus the sum of k_{cleave} and k_{ligate}. One standard approach to separate these rate constants is to measure the initial rates of cleavage (or ligation) before any significant population of product has formed. Thus in the cleavage experiment the initial rate of product formation is k_{cleave}[R·S]. Unfortunately, it was not possible to accurately determine [R·S] here since this would require knowing the concentration of the *active* ribozyme-substrate species. For example, if only 50% of the ribozyme−substrate complexes are active, the k_{cleave} determined by this initial rate method would be a factor of 2 smaller than the true k_{cleave}. Under some conditions a factor of 2 error in the rate constant would not significantly affect the analysis, but it has a large impact here because k_{cleave} and k_{ligate} have similar values (Table 1).

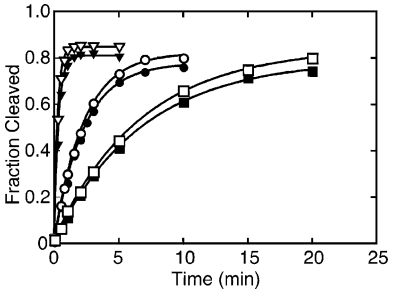

FIGURE 8: Single turnover cleavage kinetics for the cave cricket hammerheads. A plot of the fraction of cleaved substrate vs time for *D. baccettii* (solid symbols) and *D. schiavazzi*i (open symbols) cricket hammerhead constructs at 0.5 mM (squares), 1 mM (circles), and 5 mM (triangles) Mg^{2+}.

Comparison of the Schistosoma Hammerhead with Other Ribozymes. To determine the effect of the loop−loop tertiary interaction on the cleavage and ligation rate constants, a *Schistosoma* control was designed that disrupted the loop−loop tertiary interaction between stems I and II by altering the loop sequence of stem II to UUCG. This control has a $k_{obs,cleave}$ of $\sim$0.03 min^{-1} in 10 mM Mg^{2+}, which is much smaller than the $\sim$1 min^{-1} for the minimal hammerhead under the same conditions (*27*). It has previously been observed that increasing the length of stem II to greater than four base pairs reduces the rate of cleavage in the minimal hammerhead $\sim$5-fold (*50*). Thus the longer stem II for the UUCG control appears to inhibit cleavage compared to the minimal hammerhead. Thus, we chose to compare the rate constants determined here for the *Schistosoma* to the rate constants observed in the well-characterized minimal construct, HH16 (*27*). The loop−loop tertiary interaction of the *Schistosoma* hammerhead ribozyme leads to an $\sim$20-fold increase in the cleavage rate constant and an $\sim$2000-fold increase in the ligation rate constant compared to HH16.

We also studied the kinetics of hammerhead constructs derived from RNA transcripts of satellite DNAs of two cave cricket species (*51*), *Dolichopoda baccettii* and *Dolichopoda schiavazzii* (Figure S1A). Cleavage experiments were performed under identical conditions as used with the *Schistosoma* constructs, and both cricket constructs cleaved $\sim$80% of their respective substrates with $k_{obs,cleave}$ of $\sim$0.15 min^{-1} in 0.5 mM Mg^{2+}, $\sim$0.4 min^{-1} in 1 mM Mg^{2+}, and $\sim$3 min^{-1} in 5 mM Mg^{2+} (Figure 8). These values are 10−20-fold smaller than the $k_{obs,cleave}$ values determined for Schist26 under the same Mg^{2+} concentrations and are closer to cleavage rates for the minimal hammerhead (*27*). To determine the effect of the loop−loop tertiary interaction in these cave cricket constructs, the loop sequences in stem II were change to UUCG (Figure S1A) as in the *Schistosoma*

control construct. When disrupting the loop−loop tertiary interaction, both cave cricket hammerheads show $k_{obs,cleave}$ in 10 mM Mg^{2+} of ~0.03 min^{-1} (data not shown). This is the same rate constant observed for the *Schistosoma* UUCG control and 30-fold smaller than 1 min^{-1} for HH16, again most likely due to the longer stem II. Thus, although these cave cricket constructs are slower than the *Schistosoma* constructs, the loop−loop tertiary interactions increase the cleavage rate compared to the UUCG controls. Ligation experiments were performed at 1 mM Mg^{2+} on the cave cricket hammerhead ribozymes, but no ligated product was detected (the detection limit is >0.2% ligated; data not shown). Native gels on the ligation constructs indicated that the 3′ product may not have been annealing to the ribozyme strand. Thus, the sequence in stem I was redesigned to reduce the possibility of self-structure in the 3′ product, P2, but again no ligated product was detected. These results provide a lower limit on the internal equilibrium for these natural hammerhead ribozymes, where using the observed plateau in the cleavage experiments gives a $K_{eq}^{int} \geq 4$.

Hammerhead ribozymes derived from the positive and negative strands of the ASBVd (*14*) were also studied here, and both cleaved to a high percentage: >80% cleaved in 5 mM Mg^{2+}, with $k_{obs,cleave}$ values for ASBVd(+) and ASBVd(−) 6-fold and 25-fold smaller, respectively, than those measured for the *Schistosoma* hammerhead (Figure S1B for constructs; data not shown). Controls that disrupted the loop−loop tertiary interactions were made by base pairing the internal loop in stem II to create a continuous helix (Figure S1B). In 5 mM Mg^{2+} the controls for ASBVd(+) and ASBVd(−) show an ~5-fold and ~15-fold decrease, respectively, in $k_{obs,cleave}$ compared to their wild-type constructs, showing that the loop−loop tertiary interaction still has an effect on the observed cleavage rate. As observed for the cave cricket hammerheads, no ligation activity was detected in 1 mM Mg^{2+}. One possibility for the lack of ligation in the ASBVd and cave cricket constructs studied here is that there may be a high percentage of inactive species in the ligation constructs for these ribozymes. Another possibility is that some hammerhead systems may require additional sequences and/or a host factor for full activity. For example, an avocado chloroplast RNA-binding protein has been shown to accelerate self-cleavage of the ASBVd(+) hammerhead in vitro (*19*). Furthermore, not all hammerhead ribozymes may be required to perform both cleavage and ligation activities in vivo (*20*). Although monomeric (−) circular RNA has been found in ASBVd-infected avocados (*52*), it is not known whether the self-cleaved RNA monomers in the cave crickets or *Schistosomes* are circularized in vivo (*51*). The role of hammerhead ribozymes in salamanders, cave crickets and *Schistosomes* has yet to be determined (*53*).

This *Schistosoma* hammerhead construct shows a significantly higher fraction of ligated substrate (~20%) than other hammerhead ribozyme constructs reported to date with a K_{eq}^{int} of ~3 in 1 mM Mg^{2+} and ~1.5 in 10 mM Mg^{2+}. HH16 has a K_{eq}^{int} of 130 in 10 mM Mg^{2+} (*27*). However, when a minimal hammerhead was chemically cross-linked to help bring stems I and II together, the fraction of ligated substrate increased dramatically to a K_{eq}^{int} of ~1 (*54*). This change in K_{eq}^{int} was achieved by an ~100-fold increase in the ligation rate with little change in the cleavage rate, whereas the *Schistosoma* hammerhead shows increases in both the ligation and cleavage rates. Thus the cross-link between stems I and II only partially mimics the effects of the loop−loop tertiary interaction between these stems in the natural hammerhead systems. The sTRSV natural hammerhead also shows a higher fraction of ligated substrate than the minimal hammerhead, with K_{eq}^{int} ~16 in 1 mM Mg^{2+} and 7.3 in 10 mM Mg^{2+} (*32*). Previous studies on a *Schistosoma* construct similar to the ones used here reach a maximum of 6% ligated substrate (with a reported K_{eq}^{int} of 17 at 1 mM Mg^{2+}) (*39*). Thus all of the natural hammerheads have lower values of K_{eq}^{int} than the minimal construct. This smaller internal equilibrium constant is consistent with the proposed dual roles of cleavage and ligation for some hammerhead ribozymes in vivo.

The hammerhead ribozyme is classified as a small nucleolytic ribozyme along with the hairpin, VS, and HDV ribozymes (*55*). All of these ribozymes are thought to be involved in the processing of replication intermediates, but they show quite different internal equilibrium constants. The minimal hairpin ribozyme with two-way helical junction favors ligation with a K_{eq}^{int} of ~0.16, and the natural four-way helical junction hairpin ribozyme from sTRSV favors ligation even more with a K_{eq}^{int} ~0.033 (*49*). This difference in K_{eq}^{int} between the two-way and four-way junction was achieved by an increase in the ligation rate with no change in the cleavage rate. Single molecule studies independently determined a K_{eq}^{int} of 0.029 for the four-way hairpin (*56*). In contrast to these other ribozymes, the HDV ribozyme is thought to be a dedicated nuclease since no ligation activity has been detected under physiological conditions (*57*). The minimal construct of the VS ribozyme also lacks detectable ligation activity; however, extending the natural sequence revealed a region of complementarity 5′ and 3′ of the minimal self-cleaving domain that promotes the ligation reaction in vitro (*58*).

CONCLUSION

The well-characterized natural *Schistosoma* hammerhead ribozyme has been shown here to be efficient at both cleavage and ligation of RNA substrates in vitro. Formation of the loop−loop tertiary interaction in this natural hammerhead has a large effect on catalytic activity leading to ~20-fold and ~2000-fold increases in the cleavage and ligation rates, respectively, compared to the minimal hammerhead. Thus, under physiological conditions in vitro this ribozyme has similar rate constants for cleavage and ligation and shows a slight preference for cleaved versus ligated product, with a K_{eq}^{int} of 2−3 at 0.1−1 mM Mg^{2+}. The Mg^{2+} dependence of the cleavage kinetics shows saturation of k_{cleave} above ~30 mM, indicating that there is a change in the rate-limiting step for the cleavage reaction as a function of Mg^{2+} concentration. k_{ligate} shows no evidence of saturation even at 50 mM Mg^{2+} so that the rate-limiting step for ligation is Mg^{2+} dependent over a wider range of Mg^{2+} concentrations (0.1−50 mM). These results illustrate the importance of measuring both the ligation and cleavage kinetics in the hammerhead ribozymes.

Peracchi et al. proposed a model where the hammerhead ribozyme exists in multiple conformations in solution, but only a subset of these conformations are catalytically active

(*59*). Nelson and Uhlenbeck extended this model on the basis of the crystal structure of the *Schistosoma* hammerhead where formation of the loop−loop tertiary interaction leads to a higher population of catalytically active molecules, resulting in higher catalytic activity for the ribozyme (*30*). The kinetic data here support this model where the large increase in apparent k_{ligate} for the natural versus minimal hammerhead does not result from a change in k_{cat} but, instead, arises from a higher population of catalytically active molecules in solution. Ensemble FRET has been used to study global folding of a natural hammerhead ribozyme that contains the loop−loop tertiary interaction (*35*). These studies employed noncleavable substrates and so primarily give information about how this tertiary interaction affects folding prior to the cleavage reaction. Analogous studies on a cleaved substrate−ribozyme complex should also provide useful information on how the loop−loop tertiary interaction affects the folding of the cleaved hammerhead (J. Boots and A. Pardi, unpublished results). Single molecule FRET studies could prove even more informative, where it may be possible to determine both the populations and lifetimes of the catalytically active species in the hammerhead systems, analogous to recent single molecule studies on the hairpin ribozyme (*60*). Additionally, it would be interesting to see if the crystal structure of a cleaved natural hammerhead will have a conformation similar to that of the uncleaved hammerhead, since for the *Schistosoma* hammerhead the ligation reaction is nearly as efficient as the cleavage reaction.

ACKNOWLEDGMENT

We thank Dr. Olke Uhlenbeck, Dr. Chris Downey, and Michael Latham for valuable discussions.

SUPPORTING INFORMATION AVAILABLE

The constructs used in the kinetics experiments for the cave cricket and ASBVd hammerhead ribozymes (Figure S1). This material is available free of charge via the Internet at http://pubs.acs.org.

REFERENCES

1. Steitz, T. A., and Moore, P. B. (2003) RNA, the first macromolecular catalyst: the ribosome is a ribozyme, *Trends Biochem. Sci. 28*, 411−418.
2. Bashan, A., Agmon, I., Zarivach, R., Schluenzen, F., Harms, J., Berisio, R., Bartels, H., Franceschi, F., Auerbach, T., Hansen, H. A. S., Kossoy, E., Kessler, M., and Yonath, A. (2003) Structural basis of the ribosomal machinery for peptide bond formation, translocation, and nascent chain progression, *Mol. Cell 11*, 91−102.
3. Kruger, K., Grabowski, P. J., Zaug, A. J., Sands, J., Gottschling, D. E., and Cech, T. R. (1982) Self-splicing RNA−Auto-excision and auto-cyclization of the ribosomal-RNA intervening sequence of Tetrahymena, *Cell 31*, 147−157.
4. Peebles, C. L., Perlman, P. S., Mecklenburg, K. L., Petrillo, M. L., Tabor, J. H., Jarrell, K. A., and Cheng, H. L. (1986) A self-splicing RNA excises an intron lariat, *Cell 44*, 213−223.
5. Vanderveen, R., Arnberg, A. C., Vanderhorst, G., Bonen, L., Tabak, H. F., and Grivell, L. A. (1986) Excised group-II introns in yeast mitochondria are lariats and can be formed by self-splicing in vitro, *Cell 44*, 225−234.
6. Guerriertakada, C., Gardiner, K., Marsh, T., Pace, N., and Altman, S. (1983) The RNA moiety of ribonuclease-P is the catalytic subunit of the enzyme, *Cell 35*, 849−857.
7. Frank, D. N., and Pace, N. R. (1998) Ribonuclease P: Unity and diversity in a tRNA processing ribozyme, *Annu. Rev. Biochem. 67*, 153−180.
8. Winkler, W., Nahvi, A., Roth, A., Collins, J., and Breaker, R. (2004) Control of gene expression by a natural metabolite-responsive ribozyme, *Nature 428*, 263−264.
9. Symons, R. H. (1997) Plant pathogenic RNAs and RNA catalysis, *Nucleic Acids Res. 25*, 2683−2689.
10. Flores, R., Delgado, S., Gas, M. E., Carbonell, A., Molina, D., Gago, S., and De la Pena, M. (2004) Viroids: the minimal non-coding RNAs with autonomous replication, *FEBS Lett. 567*, 42−48.
11. Prody, G. A., Bakos, J. T., Buzayan, J. M., Schneider, I. R., and Bruening, G. (1986) Autolytic processing of dimeric plant-virus satellite RNA, *Science 231*, 1577−1580.
12. Branch, A. D., and Robertson, H. D. (1984) A replication cycle for viroids and other small infectious RNAs, *Science 223*, 450−455.
13. Flores, R., Hernandez, C., de la Pena, M., Vera, A., and Daros, J. A. (2001) Hammerhead ribozyme structure and function in plant RNA replication, *Methods Enzymol. 341*, 540−552.
14. Hutchins, C. J., Rathjen, P. D., Forster, A. C., and Symons, R. H. (1986) Self-cleavage of plus and minus RNA transcripts of Avocado sunblotch viroid, *Nucleic Acids Res. 14*, 3627−3640.
15. Forster, A. C., and Symons, R. H. (1987) Self-cleavage of plus and minus RNAs of a virusoid and a structural model for the active-sites, *Cell 49*, 211−220.
16. Buzayan, J. M., Hampel, A., and Bruening, G. (1986) Nucleotide-sequence and newly formed phosphodiester bond of spontaneously ligated satellite tobacco ringspot virus-RNA, *Nucleic Acids Res. 14*, 9729−9743.
17. Cote, F., and Perreault, J. P. (1997) Peach latent mosaic viroid is locked by a 2′,5′-phosphodiester bond produced by in vitro self-ligation, *J. Mol. Biol. 273*, 533−543.
18. Cote, F., Levesque, D., and Perreault, J. P. (2001) Natural 2′,5′-phosphodiester bonds found at the ligation sites of peach latent mosaic viroid, *J. Virol. 75*, 19−25.
19. Daros, J. A., and Flores, R. (2002) A chloroplast protein binds a viroid RNA in vivo and facilitates its hammerhead-mediated self-cleavage, *EMBO J. 21*, 749−759.
20. Branch, A. D., Robertson, H. D., Greer, C., Gegenheimer, P., Peebles, C., and Abelson, J. (1982) Cell-free circularization of viroid progeny RNA by an RNA ligase from wheat-germ, *Science 217*, 1147−1149.
21. Baumstark, T., Schroder, A. R. W., and Riesner, D. (1997) Viroid processing: Switch from cleavage to ligation is driven by a change from a tetraloop to a loop E conformation, *EMBO J. 16*, 599−610.
22. Tsagris, M., Tabler, M., Muhlbach, H. P., and Sanger, H. L. (1987) Linear oligomeric potato spindle tuber viroid (PSTV) RNAs are accurately processed in vitro to the monomeric circular viroid proper when incubated with a nuclear extract from healthy potato cells, *EMBO J. 6*, 2173−2183.
23. Fedor, M. J., and Williamson, J. R. (2005) The catalytic diversity of RNAs, *Nat. Rev. Mol. Cell Biol. 6*, 399−412.
24. Uhlenbeck, O. C. (1987) A small catalytic oligoribonucleotide, *Nature 328*, 596−600.
25. Forster, A. C., and Symons, R. H. (1987) Self-cleavage of virusoid RNA is performed by the proposed 55-nucleotide active-site, *Cell 50*, 9−16.
26. Blount, K. E., and Uhlenbeck, O. C. (2005) The structure-function dilemma of the hammer head ribozyme, *Annu. Rev. Biophys. Biomol. Struct. 34*, 415−440.
27. Hertel, K. J., Herschlag, D., and Uhlenbeck, O. C. (1994) A kinetic and thermodynamic framework for the hammerhead ribozyme reaction, *Biochemistry 33*, 3374−3385.
28. Khvorova, A., Lescoute, A., Westhof, E., and Jayasena, S. D. (2003) Sequence elements outside the hammerhead ribozyme catalytic core enable intracellular activity, *Nat. Struct. Biol. 10*, 708−712.
29. De la Pena, M., Gago, S., and Flores, R. (2003) Peripheral regions of natural hammerhead ribozymes greatly increase their self-cleavage activity, *EMBO J. 22*, 5561−5570.
30. Nelson, J. A., and Uhlenbeck, O. C. (2006) When to believe what you see, *Mol. Cell 23*, 447−450.
31. Canny, M. D., Jucker, F. M., Kellogg, E., Khvorova, A., Jayasena, S. D., and Pardi, A. (2004) Fast cleavage kinetics of a natural hammerhead ribozyme, *J. Am. Chem. Soc. 126*, 10848−10849.
32. Nelson, J. A., Shepotinovskaya, I., and Uhlenbeck, O. C. (2005) Hammerheads derived from sTRSV show enhanced cleavage and ligation rate constants, *Biochemistry 44*, 14577−14585.

33. Ferbeyre, G., Smith, J. M., and Cedergren, R. (1998) Schistosome satellite DNA encodes active hammerhead ribozymes, *Mol. Cell. Biol. 18*, 3880−3888.
34. Chartrand, P., Harvey, S. C., Ferbeyre, G., Usman, N., and Cedergren, R. (1995) An oligodeoxyribonucleotide that supports catalytic activity in the hammerhead ribozyme domain, *Nucleic Acids Res. 23*, 4092−4096.
35. Penedo, J. C., Wilson, T. J., Jayasena, S. D., Khvorova, A., and Lilley, D. M. J. (2004) Folding of the natural hammerhead ribozyme is enhanced by interaction of auxiliary elements, *RNA 10*, 880−888.
36. Kim, N. K., Murali, A., and DeRose, V. J. (2005) Separate metal requirements for loop interactions and catalysis in the extended hammerhead ribozyme, *J. Am. Chem. Soc. 127*, 14134−14135.
37. Heckman, J. E., Lambert, D., and Burke, J. M. (2005) Photocrosslinking detects a compact, active structure of the hammerhead ribozyme, *Biochemistry 44*, 4148−4156.
38. Lambert, D., Heckman, J. E., and Burke, J. M. (2006) Three conserved guanosines approach the reaction site in native and minimal hammerhead ribozymes, *Biochemistry 45*, 7140−7147.
39. Osborne, E. M., Schaak, J. E., and DeRose, V. J. (2005) Characterization of a native hammerhead ribozyme derived from schistosomes, *RNA 11*, 187−196.
40. Martick, M., and Scott, W. G. (2006) Tertiary contacts distant from the active site prime a ribozyme for catalysis, *Cell 126*, 309−320.
41. Milligan, J. F., Groebe, D. R., Witherell, G. W., and Uhlenbeck, O. C. (1987) Oligoribonucleotide synthesis using T7 RNA-polymerase and synthetic DNA templates, *Nucleic Acids Res. 15*, 8783−8798.
42. Stage-Zimmermann, T. K., and Uhlenbeck, O. C. (1998) Hammerhead ribozyme kinetics, *RNA 4*, 875−889.
43. Fedor, M. J., and Uhlenbeck, O. C. (1990) Substrate sequence effects on hammerhead RNA catalytic efficiency, *Proc. Natl. Acad. Sci. U.S.A. 87*, 1668−1672.
44. Herschlag, D. (1995) RNA chaperones and the RNA folding problem, *J. Biol. Chem. 270*, 20871−20874.
45. Uhlenbeck, O. C. (1995) Keeping RNA happy, *RNA 1*, 4−6.
46. Hertel, K. J., Peracchi, A., Uhlenbeck, O. C., and Herschlag, D. (1997) Use of intrinsic binding energy for catalysis by an RNA enzyme, *Proc. Natl. Acad. Sci. U.S.A. 94*, 8497−8502.
47. Serra, M. J., and Turner, D. H. (1995) Predicting thermodynamic properties of RNA, *Methods Enzymol. 259*, 242−261.
48. Bloomfield, V. A., Crothers, D. M., and Tinoco, I. (2000) Double helix formation by oligonucleotides without loops, in *Nucleic Acids: Structures, Properties, and Functions* (Steifel, J., Ed.) pp 271−291, University Science Books, Sausalito, CA.
49. Fedor, M. J. (1999) Tertiary structure stabilization promotes hairpin ribozyme ligation, *Biochemistry 38*, 11040−11050.
50. Clouet-d'Orval, B., and Uhlenbeck, O. C. (1997) Hammerhead ribozymes with a faster cleavage rate, *Biochemistry 36*, 9087−9092.
51. Rojas, A. A., Vazquez-Tello, A., Ferbeyre, G., Venanzetti, F., Bachmann, L., Paquin, B., Sbordoni, V., and Cedergren, R. (2000) Hammerhead-mediated processing of satellite pDo500 family transcripts from *Dolichopoda* cave crickets, *Nucleic Acids Res. 28*, 4037−4043.
52. Daros, J. A., Marcos, J. F., Hernandez, C., and Flores, R. (1994) Replication of Avocado sunblotch viroid—Evidence for a symmetrical pathway with 2 rolling circles and hammerhead ribozyme processing, *Proc. Natl. Acad. Sci. U.S.A. 91*, 12813−12817.
53. Ugarkovic, D. (2005) Functional elements residing within satellite DNAs, *EMBO Rep. 6*, 1035−1039.
54. Stage-Zimmermann, T. K., and Uhlenbeck, O. C. (2001) A covalent crosslink converts the hammerhead ribozyme from a ribonuclease to an RNA ligase, *Nat. Struct. Biol. 8*, 863−867.
55. Lilley, D. M. J. (2001) Origins of RNA catalysis in the hairpin ribozyme, *ChemBioChem 2*, 729−733.
56. Nahas, M., Wilson, T. J., Hohng, S. C., Jarvie, K., Lilley, D. M. J., and Ha, T. (2004) Observation of internal cleavage and ligation reactions of a ribozyme, *Nat. Struct. Mol. Biol. 11*, 1107−1113.
57. Taylor, J. M. (2003) Replication of human hepatitis delta virus: recent developments, *Trends Microbiol. 11*, 185−190.
58. Jones, F. D., Ryder, S. P., and Strobel, S. A. (2001) An efficient ligation reaction promoted by a varkud satellite ribozyme with extended 5′ and 3′-termini, *Nucleic Acids Res. 29*, 5115−5120.
59. Peracchi, A., Karpeisky, A., Maloney, L., Beigelman, L., and Herschlag, D. (1998) A core folding model for catalysis by the hammerhead ribozyme accounts for its extraordinary sensitivity to abasic mutations, *Biochemistry 37*, 14765−14775.
60. Zhuang, X. W., Kim, H., Pereira, M. J. B., Babcock, H. P., Walter, N. G., and Chu, S. (2002) Correlating structural dynamics and function in single ribozyme molecules, *Science 296*, 1473−1476.

BI062077R